AIIM

Association for Information and Image Management

1100 Wayne Avenue, Suite 1100
Silver Spring, Maryland 20910

301/587-8202

Centimeter

Inches

MANUFACTURED TO AIIM STANDARDS
BY APPLIED IMAGE, INC.

1 of 1

CONF-940524--4 ANL/TD/CP--82610

ILLICIT SUBSTANCE DETECTION USING FAST-NEUTRON TRANSMISSION SPECTROSCOPY

B. J. Micklich, M. K. Harper, A. H. Novick, and D. L. Smith
Technology Development Division, Argonne National Laboratory, Argonne, Illinois 60439 USA

Fast-neutron interrogation techniques are of interest for detecting illicit substances such as explosives and drugs because of their ability to identify light elements such as carbon, nitrogen, and oxygen. Fast-Neutron Transmission Spectroscopy (FNTS) uses standard time-of-flight techniques to measure the energy spectrum of neutrons emitted from a collimated continuum source before and after transmission through the interrogated sample. The Monte Carlo transport code MCNP is used to model fast-neutron transmission experiments using a ^{9}Be(d,n) source [E_d = 5 MeV]. The areal densities (number of atoms per cm^2), and the uncertainties, of various elements present in the sample are determined by an unfolding algorithm which includes the effects of cross-section errors and correlations. Results are displayed in the form of normalized densities, including their errors and correlations, which are then compared to the values for explosives and benign substances. Probabilistic interpretations of the results are discussed in terms of substance detection and identification.

1. Introduction

Fast-neutron interrogation techniques are being studied for the detection of illicit substances (e.g., explosives and drugs). These techniques offer the possibility of determining the densities, or their ratios, of light elements such as carbon, nitrogen, and oxygen, which are the primary constituents of these materials. Explosives and drugs have densities of these three elements which distinguish them from most benign substances. Fast-Neutron Transmission Spectroscopy (FNTS) uses standard time-of-flight (TOF) techniques to measure the energy spectrum of neutrons emitted from a collimated continuum source before and after transmission through the interrogated sample. The basic technique was pioneered by Overley [1,2] for bulk material analysis. An unfolding algorithm determines the areal densities (number density per cm^2), and their uncertainties, of various elements present in the sample. The results are then normalized to total number densities which can be used to determine the presence of illicit substances. An accurate treatment of errors throughout the analysis allows a probabilistic interpretation of these quantities.

2. Monte Carlo Modeling

The Monte Carlo transport code MCNP [3] was used to simulate transmission experiments. The calculational model assumes a collimated parallel neutron beam irradiating the object being interrogated. The neutron source used is the zero-degree neutron energy spectrum from the ^{9}Be(d,n) reaction at E_d = 5 MeV. This deuteron energy results in a source with high neutron yield in the range 1-4 MeV, which contains many resolved resonances for the light elements. The source-detector distance is taken to be 5 m, with source and detector timing widths of 2 nsec. Analog particle transport was used (i.e., no variance reduction) so that each neutron from the source represents one neutron from a real source in an experimental or test geometry. In this way we can achieve errors of the proper magnitude and variation across energy phase space, which is important in evaluating analysis and decision-making algorithms that use the data. Detector efficiency in each time/energy bin (ε_i) is accounted for by scaling the simulated detector counts (N_i) and fractional standard deviation (σ_i) by

$$N_i = N_i \cdot \varepsilon_i \quad \text{and} \quad \sigma_i = \sigma_i / \sqrt{\varepsilon_i}\,, \qquad (1)$$

the latter being equivalent to assuming $\sigma_i^2 = N_i$.

The number of neutron histories required to simulate a given set of exposure conditions is calculated with the equation

$$R/(\langle T\rangle \langle \varepsilon\rangle) = \text{source n/s} = S_n\, \Delta\Omega\, I_p\, \tau_p\, f \qquad (2)$$

where R = maximum detector count rate
$\langle T\rangle$ = average transmission
$\langle \varepsilon\rangle$ = average detector efficiency
S_n = zero-degree neutron emission (n/sr-s-μC)

$\Delta\Omega$ = detector solid angle (sr)
I_p = pulse current (μA)
τ_p = pulse time width (s)
f = accelerator pulse repetition rate (1/s)

so that for given values of <T>, <ε>, source parameters, and geometry, one can calculate the required number of neutron histories. For example, using the information given earlier and assuming <T> = 0.48, <ε> = 0.15, f = 1 MHz, a count rate of 10^5/s, and a detector diameter of 10 cm, we find that I_p = 1.2 mA and that a 1-s irradiation would correspond to about 1.4 million neutrons emitted toward the detector.

3. Unfolding Algorithm

The transmission data are analyzed in the time domain using standard nuclear techniques [4] adapted to the method of effective variance.[5] The details of the algorithm are contained in References [6] and [7]. The cross-section data used in the inversion process are obtained by simulating transmission experiments for pure elements, and inverting the transmission results to get the cross sections. Three different elemental sets are used: two ten-element sets consisting of [H C N O F Al Si Cl Fe Cu] and [H C N O F Na Si Cl K X], where X is a fictitious element meant to account for those elements not explicitly included; and one five-element set consisting of [H C N O X]. The ten element sets are chosen to include the elements present in most conventional high explosives [H C N O]; elements which are present in many non-nitrogen-based explosives [F Na Si Cl K]; and other elements which we might reasonably expect to find inside luggage [Al Si Fe Cu]. The element X is given a flat cross section. The results are expressed as normalized densities, which are the ratios of the elemental areal densities to total areal density (of all elements present), which removes the unknown sample thickness.

Errors are propagated throughout the calculation, so that the qualifiers are presented with errors and correlations. This allows us to present results in the form of Figure 1. Shown are the solution point (as a +) and the locus of points which lie one standard deviation away from the solution: this ellipse is called the 1-σ curve. The effect of the second iteration through the algorithm is to refine the estimate of areal densities and to increase the standard deviation, since now cross-section errors are being taken into account. The solution point will not always move closer to the true value, but it will be closer in a statistical sense since the standard deviation is larger.

4. Results

The unfolding algorithm has been tested in collimated geometry for a number of materials to determine whether it is capable of giving reliable results. The stability of the algorithm is shown in Figure 2, which shows the results of ten independent runs for 3 cm thickness of the high explosive RDX, each equivalent to a one-second exposure. The solutions all cluster around the true solution point and nearly all include the true solution within the 1-σ curve.

Figure 3 shows the results for various thicknesses of RDX from 3 to 20 cm, all using the same number of neutron histories. Because of collimation, even the thickest samples show good resolution in the time/energy spectrum so that good unfolding results are obtained. The average transmission for 3-cm thickness is about 0.52, while for 20 cm thickness it is about 0.02. The standard deviations initially decrease with thickness, are smallest for 8 cm, and then increase at the greater thicknesses. This effect agrees with results [8] that indicate that the optimum transmission for exponential attenuation measurements is 0.1-0.3. The fractional standard deviation for energy bins in the 1-4 MeV range is about 1% for 3 cm thickness, 1.8% for 8 cm thickness, and about 6.6% for 20 cm thickness.

Transmission results were also obtained for various materials composed of the elements listed in Section 3, and others, to test the algorithm's ability to unfold accurately the areal densities of a variety of elements. A variety of materials have been simulated, singly or in combination. The list includes such materials as ABS plastic, water, various explosives (including some which are not nitrogen-based), melamine, polyurethane, glass, plexiglas, cloth, salt, sugar, etc. The areal densities calculated for a given material or combination of materials are quite good, as long as the constituent elements are represented in the cross-section matrix used in the unfolding algorithm.

As an example, consider cases with the metals Al, Fe, and Cu, both alone and combined with water in a 50% by volume mixture. Unfolding using the cross-section set containing these metals yields very accu-

rate results for the areal densities, including no density for elements not present. When using the second ten-element set, the metal density is not assigned to X, but is spread among several elements. In addition, where the water contribution is analyzed well for the first set, with the second set not even this contribution is determined correctly. Part of the problem may be that a flat cross section is not a good representation for the medium-weight nuclei, which tend to have total cross sections which decrease with energy, on the average, over the range 1-10 MeV.

Counting statistics are best for energy bins in the 1-4 MeV range, owing to the energy dependences of the neutron source and typical neutron detector efficiencies. The unfolding algorithm was tested using only that part of the spectrum. Using the repeated trials of RDX, unfolding with all time bins gave qualifier results which were closer to the true values. Thus the bins outside the 1-4 MeV range still contribute valuable information even though the statistics are poorer. Some analysis was also performed using only the five element set; this gave better results for normalized N and O than did the ten-element set when the entire energy range was used, and about the same results using the energy range 1-4 MeV.

Uncollimated geometries were also modeled to study the effects of small-angle scattering. The primary effect would be spectral distortion since neutrons arriving at any given time may have different energies. The cases involved broad-beam irradiation of samples viewed by an uncollimated detector. These cases yielded only a few percent scattered neutrons at most, which does not distort the spectrum enough to markedly change the areal densities or the qualifiers. These results suggest that multiple scattering within the sample is not inportant, and that scattering effects may be dominated by the surrounding materials (walls, detector shielding, etc.). One reason for looking at the ratios of areal densities is that, since the effect of scattered neutrons is to create an apparently larger density, this effect might be reduced or eliminated by taking ratios of two quantities which are both increased by scattering.

5. Interpretation of Qualifiers

The areal or projected densities which result from the unfolding analysis provide the input into a decision algorithm to determine the presence of an explosive. One can look at elemental areal densities, normalized areal densities, or some probabilistic interpretation of these quantities. Such a probabilistic interpretation can be provided by integrating the probability density that arises from the unfolding algorithm over some region of phase space that is "explosive-like", or by testing the hypothesis that an explosive is present.[7] For each of these quantities, we have the choice of looking at a single projection, looking at multiple (say, two or three) projections independently, or combining the data from several projections in a tomographic reconstruction of the object. We are currently investigating the analysis of projection data, including the use of pattern-recognition software for determining the presence of explosives. We are also exploring the requirements of few-view tomographic reconstruction for this application, and evaluating the number and nature of projections required, the quantities to be reconstructed, and the reconstruction algorithms which give acceptable results.

6. Conclusions and Future Directions

We plan to make refinements to the unfolding algorithm, in particular investigating the effects of constraining the algorithm with regard to negative or statistically insignificant results for densities. Many more simulations will be performed and analyzed for uncollimated geometries. This may require additional source measurements of the energy spectrum and yield at angles other than zero degrees. This will lead to models for larger objects (i.e., suitcases) which will generate data that can be analyzed using radiographic or few-view tomographic techniques.

Acknowledgments

This work was supported by the Federal Aviation Administration Technical Center under contract DTFA03-03-X-00021. M. K. Harper was supported by the Student Research Participation Program of Argonne's Division of Educational Programs.

References

[1] J. C. Overley, *J. Appl. Radiat. Isot.* **36**, pp 185-191 (1985).

[2] J. C. Overley, *Nucl. Instr. Meth.* **B24/25**, pp. 1058-1062 (1987).

[3] 'MCNP - A Generalized Monte Carlo Code for Neutron and Photon Transport, Version 3A," LA-7396-M, Rev. 2, Los Alamos National Laboratory (Sept. 1986).
[4] D. L. Smith, ANL/NDM-62 (Nov. 1982).
[5] J. Orear, *Amer. J. Phys.* **50**, pp. 912-916 (1982).
[6] B. J. Micklich, M. K. Harper, L. Sagalovsky, and D. L. Smith, Int'l Conf. on Nuclear Data for Science and Technology, Gatlinburg, TN (May 1994).
[7] D. L. Smith, L. Sagalovsky, B. J. Micklich, M. K. Harper, and A. H. Novick, Proc. 4th Int'l Conf. on Applications of Nuclear Techniques, Crete, Greece (June 1994).
[8] E. J. Burge, *Nucl. Instr. Meth.* **144**, pp. 547-555 (1977).

Figures

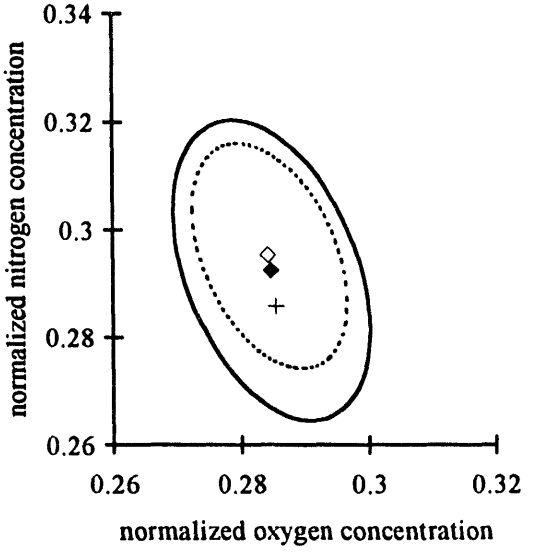

Figure 1. Solution for 3 cm thickness RDX in terms of the normalized concentrations of oxygen and nitrogen. The exposure is equivalent to a one-second exposure for the conditions described in the text (1.4 million neutron histories).

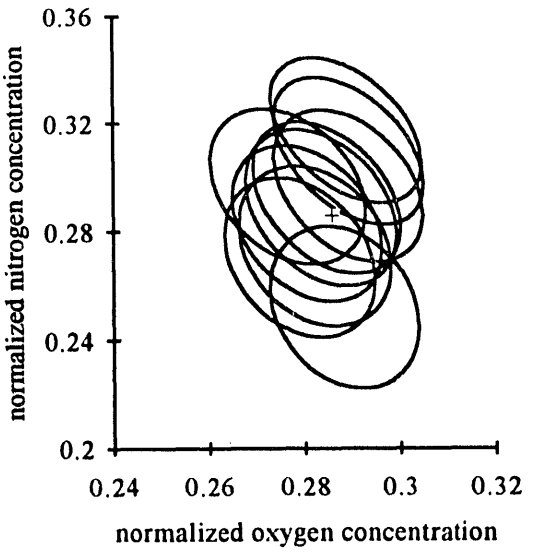

Figure 2. Results from ten independent runs of 3-cm thick RDX for a one-second exposure each. The plus sign shows the true solution and the curves are the 1-σ ellipses.

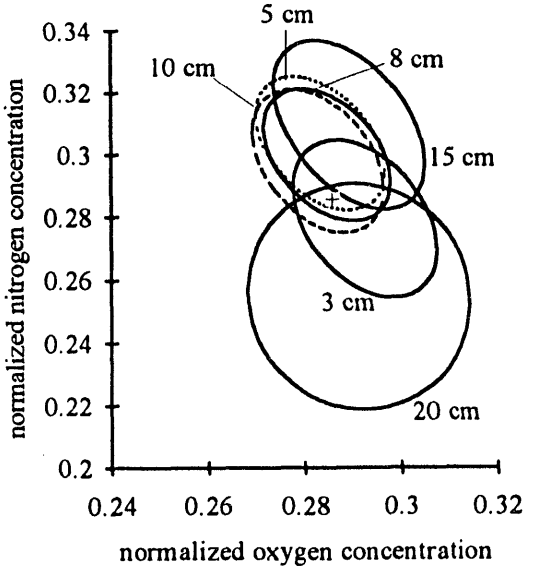

Figure 3. Solutions for various thicknesses of RDX. The true solution is shown by the plus sign, and the curves give the 1-σ ellipses.

DATE

FILMED

7/6/94

END